Article

Not peer-reviewed version

Fabrication of Fe_3O_4 Core-TiO_2/mesoSiO_2 and Fe_3O_4 Core-mesoSiO_2/TiO_2 Double Shell Nanoparticles for Methylene Blue Adsorption: Kinetic, Isotherms and Thermodynamic Characterization

Ahmed Mohamed El-Toni , Mohamed A. Habila * , Mohamed Sheikh , Mohamed El-Mahrouky , Abdulrhman S. Al-Awadi , Zeid ALOthman

Posted Date: 10 August 2023

doi: 10.20944/preprints202308.0829.v1

Keywords: magnetic core; silica shell; titnaia shell; water treatment; methylene blue; solvo-thermal process; adsorption

Article

Fabrication of Fe_3O_4 Core-TiO_2/mesoSiO_2 and Fe_3O_4 Core-mesoSiO_2/TiO_2 Double Shell Nanoparticles for Methylene Blue Adsorption: Kinetic, Isotherms and Thermodynamic Characterization

Ahmed Mohamed El-Toni [1,2], Mohamed Habila [3,*] Mohamed Sheikh [3], Mohamed El-Mahrouky [4], Abdulrhman S. Al-Awadi [5] and Zeid A. ALOthman [3]

[1] King Abdullah Institute for Nanotechnology, King Saud University, Riyadh 11451, Saudi Arabia
[2] Nanotechnology Department, Central Metallurgical Research and Development Institute (CMRDI), P.O. 87 Helwan, Cairo 11421, Egypt
[3] Chemistry Department, College of Science, King Saud University, Riyadh-11451, Saudi Arabia
[4] Soil Science Department, College of Food and Agriculture Sciences, King Saud University, Riyadh, Saudi Arabia; Eng.mas2009@gmail.com
[5] K.A. Care Energy Research and Innovation Center in Riyadh, King Saud University, Riyadh, Saudi Arabia
* Correspondence: mhabila@ksu.edu.sa; Tel.: +966-1-4674-198; Fax: +966-1-4675-992

Abstract: Wastewater treatment for removal of dyes from industrial effluents prior to discharge into the water surfaces is necessary to achieve green and sustainable environment. The continuous production and processing of dyes resulted in severe negative impacts for the ecosystem. Herein, Fe_3O_4 core-TiO_2/mesoSiO_2 and Fe_3O_4 core-mesoSiO_2/TiO_2 double shell nanoparticles were prepared by first (R1) and second (R2) routes. The structure of the fabricated Fe_3O_4 is designed to achieve coating and protection of magnetic Fe_3O_4 core and to produce double shell around to enhance the efficiency for methylene removal by adsorption process. The reported adsorption capacities for R1-0.2, R1-0.4 and R2 samples were 46, 38 and 50 mg/g respectively which obtained after 80 min as equilibrium contact time at pH of 6, using methylene blue concentration of 50 ppm. The adsorption of methylene blue using the prepared Fe_3O_4core-meso SiO_2/TiO_2 double shell was analyzed by kinetic and isotherms models. In addition, the thermodynamic investigations are applied to assess the spontaneous nature of the process. The obtained results confirmed that the pseudo-second order model is well-fitted with the adsorption data as well as the Freundlish-isotherm assumption suggested multilayer adsorption mechanism. In addition, results of thermodynamic investigation indicated that the surfaces of Fe_3O_4 core-mesoSiO_2/TiO_2 and Fe_3O_4 core-TiO_2/mesoSiO_2 double shell exhibit spontaneous tendency to adsorb methylene blue from the aqueous solutions. These results will encourage the further application of Fe_3O_4 core-meso SiO_2/TiO_2 and Fe_3O_4 core-TiO_2/meso SiO_2 double shell for removal of broad range of contaminants from wastewater.

Keywords: magnetic Fe_3O_4; coating; wastewater purification; methylene blue; nanotechnology; adsorption-modeling

1. Introduction

The problems related to water pollution have become the most a global environmental issue during the recent decades [1–3]. These problems are owed to the excessive industrial-activities which cause continuous production of polluted liquid effluents. For example, there are many types of dyes are produced by huge amounts annually and applied in the textile fields. Part of these tremendous tones of dyes are contaminated with the discharge effluents [4,5]. These dyes are dispersed in various environmental components and cause hazard to human and animals. Furthermore, these pollutants resulted in bad esthetical view and cause significant damage to the water ecosystem [4,6,7]. Methylene blue (MB) dye is known as methylthionium chloride and classified as cationic dye [8]. The common industrial applications of methylene blue are painting and

 doi:10.20944/preprints202308.0829.v1

paper industries, textiles fabrication, pesticides production, and pharmaceuticals products [9]. The water discharge from these industrial sections contains huge amounts of methylene blue dye which spread in the environment. the exposure to methylene blue cause negative impacts on human health such as vomiting, headache, cyanosis, jaundice, quadriplegia, shock, and others [10]. A large amount of dye >7.0 mg kg^{-1} causes mental disturbance, abdominal pain and nausea [11].

Currently, the most important methods for methylene blue removal is adsorption, biodegradation, chemical oxidation, photodegradation and membrane filtration. Among these treatment methods the adsorption process has showed a unique advantage such as low cost, easy performance and high removal efficiency [12–14]. The common adsorbent materials are zinc oxide, silica and silica derived materials, alumina and carbon. The broader materials categories as adsorbents include; fly ash, manganese oxide, nickel oxide and transition metal hydroxide which poses high potential for pollution remediation by adsorption [1,15]. However, the materials in the nano-size exhibit high surface area, fast dispersion in the adsorption medium leading to promised adsorption capacity compared to the traditional materials. The limitation of the nanomaterials that reduce their applicability in real field is the need for high speed centrifuge or nanofiltration to separate the adsorbent from the adsorption medium at the end of the treatment process [16,17]. To overcome this limitation, magmatic materials are introduced as adsorbents which enable high dispersion, porous structures as well as the possibility to be separated by external magnetic field [18]. Furthermore, the magnetic based nanomaterials can be prepared in a core-shell structure which allow easy functionalization with organic and/or inorganic species. The core-shell based nanomaterials open the space for tremendous adsorbent materials with amazing ability for adsorption and separation [19–21].

Different roots have been developed to prepare the core-shell based magnetic materials, however, the application of Fe_3O_4 nanoparticles as core is the most effective due to the superior magnetic properties [22–24]. The shell structure can be prepared by various coating of silica, carbon, polymer or titania to protect the magnetic core and enable various functionalization [25–27]. Salamat *et al.* have synthetized Fe_3O_4(np)@TiO_2 shell structure for water treatment applications by photocatalytic-degradation of organic pollutants [28]. Shi *et al.* have prepared core-shell structure of Fe_3O_4@titanate using the in-situ growth and hydrothermal assisted etching for application in wastewater treatment [29]. Zheng et al. have prepared Fe_3O_4@ZIF-8 as core–shell nanostructure and recommend them for removal of methylene blue with adsorption capacity of 20.2 mg g^{-1} [30]. Saini *et al.*, have applied the Fe_3O_4@Ag/SiO_2 as core-shell with excellent adsorption properties for removal of about 99.6% of methylene blue dye from aqueous solution of pH 7, and the adsorption mechanism was agreed with Langmuir isotherm assumption reporting with maximum monolayer adsorption-capacity (Q_{max}) of 128.5 mg/g [31]. Jaseela *et al.* have prepared inorganic – organic adsorbent including TiO_2 and PVA for selective adsorption of methylene blue with removal efficiency of 97.1% of MB. The adsorption kinetic was fitted with pseudo-second order-based model [32]. Zhan *et al.*, produced Fe_3O_4-derived organic/inorganic hybrid-based adsorbent with various structured magnetic (np) by solvothermal and chemical-based co-precipitation method naming the products as S-Fe_3O_4 and C-Fe_3O_4, respectively. The magnetic materials (S-Fe_3O_4 and C-Fe_3O_4) were further functionalized by dopamine (DA) and (3-aminopropyl) triethoxysilane (KH550) to produce at the end the core-shell Fe_3O_4/poly(DA + KH550) adsorbents. The application of these materials for methylene blue removal showed adsorption capacity higher than 400.00 mg g^{-1}, with well-fitting for the pseudo-second-order kinetic model and Langmuir isotherm model [33]. Schneider *et al*. have fabricated an adsorbent-composite from Fe_3O_4@SiO_2@carbon for methylene blue removal [34]. Akbarbandari *et al*. have developed a bi-metallic and tri-metallic metal–organic frameworks (MOFs) supported on the magnetic activated carbon (MAC) were synthesized for methylene blue removal. The adsorption process was reported to follow the pseudo-second-order kinetic model and Langmuir isotherm model with maximum adsorption capacity of 66.51 and 71.43 mg/g for the bi-metallic and tri-metallic based magnetic nanocomposites, respectively [35]. However, the research are still continued to investigate the various roots for building magnetic core-shell based nanocomposites with porous structures and different shell combination of metal oxides to tune the properties of core shell

 doi:10.20944/preprints202308.0829.v1

materials and improve their performance as adsorbents. Therefore, this work aimed to investigate various roots for fabrication of Fe_3O_4core-meso SiO_2/TiO_2 double shell for methylene blue adsorption. In addition to study the kinetic, isotherms and thermodynamic properties for the adsorptive-removal of methylene blue.

2. Materials and Methods

All applied chemicals were in high purity analytical grade. Ferric chloride-hexahydrate ($FeCl_3.6H_2O$), sodium acetate, sodium citrate, ammonia solution, TBOT, TEOS and cetyltrimethylammonium bromide were obtained from Sigma-Aldrich (USA).

2.1. Synthesis of Fe_3O_4 magnetic core

Certain weight of $FeCl_3$·6H2O was dissolved in a certain volume of ethylene glycol, and then calculated amount of sodium acetate, tri-sodium citrate and polyethylene glycol were added. The mixture was vigorously and continuously stirred to ensure complete mixing, and then transferred to an autoclave made from stainless-steel and lined with Teflon and heated to around 190 °C for certain time, At the end and after reaching the room temperature, the produced Fe_3O_4 magnetic core was washed three times with ethanol, and then dried at 60 °C in an oven for approximately 6 h [36].

2.2. Synthesis of Fe_3O_4core-meso SiO_2/TiO_2 double shell nanoparticles

2.2.1. Coating with mesoporous silica

Fe_3O_4 core magnetic nanoparticles is coated with mesoporous silica shell according to the following procedure, Fe_3O_4 was dispersed in H_2O/ethanol mixture ultrasonically and then exact volume from NH_4OH added. Thereafter, specific weight from cationic surfactant (cetyltrimethylammonium bromide) is added, followed by the addition TEOS [37].

2.2.2. Titania Coating

To make a layer of titania onto the magnetic nanocores, the procedure described in the work of Jianping *et al*., [38] was applied. In details, the silica coated magnetic nanocores were dispersed in ethanol and mixed with ammonia solution under ultrasonic stirring. TBOT was then added slowly. The reaction allowed to continue 24 h under mechanical stirring. Thereafter, the formed Fe_3O_4core-SiO_2/TiO_2 double shell nanoparticles were separated from the mother solution, washed several times with de-ionized water, then with ethanol, dried, and finally calcinied at 500 ^oC for 2 h to form Fe_3O_4core-meso SiO_2/TiO_2 double shell nanoparticles.

2.3. Synthesis of multifunctional Fe_3O_4core-TiO_2/meso SiO_2 double shell nanoparticles

For fabrication of Fe_3O_4core-TiO_2/meso SiO_2 double shell nanoparticles, the titania layer was coated onto magnetic Fe_3O_4 core nanoparticle surface, then a silica coating as a second layer is made, and the samples will finally be calcined. In details, the magnetic nanocores were dispersed in ethanol and mixed with ammonia solution under ultrasonic stirring. Then TBOT is then added slowly (0.2 and 0.4 mL). The reaction was allowed to continuous mechanical stirring for 24 h. Thereafter, the produced Fe_3O_4 core-TiO_2 shell was separated from the mother solution, washed several times with de-ionized water, then with ethanol, dried, and finally calcinied at 500 ^oC for 2 h air condition. The final step for coating meso SiO_2 onto Fe_3O_4core-TiO_2 was applied according to the following procedure, Fe_3O_4@TiO2 as a core was dispersed in H_2O ultrasonically and the exact volume from NH_4OH was added. Thereafter, the cationic surfactant (cetyltrimethylammonium bromide) solution is added, followed by the addition TEOS [38]. The reaction was allowed for mechanical stirring for 6h. The formed Fe_3O_4 core-TiO_2/mesoSiO_2 double shell nanoparticles was separated from mother solution, washed with ethanol and water. Finally calcining the sample at 500 ^oC for 2 h to form Fe_3O_4 core-TiO_2/meso SiO_2 double shell nanoparticles.

2.4. Adsorptive-removal study for methylene blue

To investigate the fabricated Fe_3O_4 core-meso SiO_2/TiO_2 double shell for methylene blue uptake, the batch process was applied. A certain weight of fabricated Fe_3O_4 core-meso SiO_2/TiO_2 double shell was taken in 50 mL tube and mixed with the 25 mL of 50 ppm methylene blue dye solution. the mixture was shacked for 80 min; then the phases were separated by external magnetic field. The concentration of the methylene blue dye was measured by the Uv-Visible. Blank samples without fabricated Fe_3O_4 core-meso SiO_2/TiO_2 double shell were conducted in all experiments. the adsorption capacity (qe) was calculated from the equation (1):

$$qe = (C0-Ce).\ V/M, \quad (1)$$

where C_0 is the primary concentration of methylene blue solution, Ce is final methylene blue concentration, V represent the volume of the adsorption solution, and M is the adsorbent mass (g) (Fe_3O_4 core-meso SiO_2/TiO_2 double shell).

The procedures for the adsorption of methylene blue onto Fe_3O_4 core-meso SiO_2/TiO_2 double shell were repeated to investigate the most import factors such as pH, contact time, methylene blue dye concentration and temperature, which significantly affecting the uptake of methylene blue onto fabricated Fe_3O_4 core-meso SiO_2/TiO_2 double shell.

3. Results and discussion

3.1. Characterization of Fe_3O_4core-double shell

Multi-procedures have been applied to prepared Fe_3O_4 core-meso SiO_2/TiO_2 double shell with alternative sequence of titania and silica. In the first stage, the homogenous spherical magnetic noncore (Fe_3O_4) is obtained via solvo-thermal process which resulted in separated particle with average size between 50 nm and 100 nm (Figure 1). The obtained magnetic nanocore is applied to fabricate Fe_3O_4core-mesoSiO_2/TiO_2 double shell or Fe_3O_4core-TiO_2/mesoSiO_2 double shell.

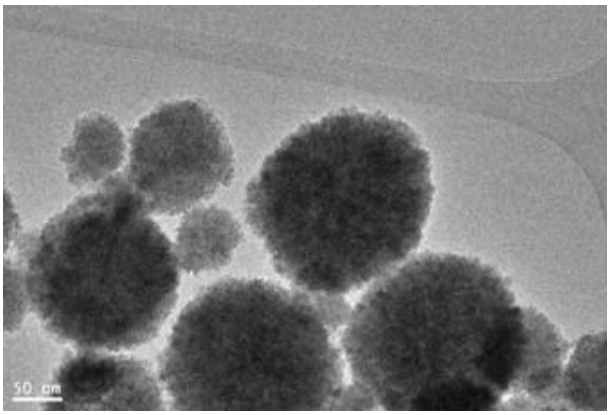

Figure 1. TEM images of Fe_3O_4 nanocores prepared by solvothermal method.

To fabricate Fe_3O_4@TiO_2@m-SiO_2, Fe_3O_4 nanoparticles using the first route. The nanoparticles were firstly coated with TiO_2 shell then secondly with mesoporous silica shell then finally calcination process is conducted to crystalize TiO_2 shell and to remove surfactant from silica shell to transform it to mesoporous one. TiO_2 coating into Fe_3O_4 nanoparticles was conducted by Stöber-modified approach where citrate modified Fe3O4 nanoparticles are dispersed in ethanol solution then ammonium hydroxide and titanium butoxide is added to the above mixture where the coating process are conducted at 45 ^oC for 20h. Mesoporous silica step was conducted onto TiO_2 coated Fe3O4 by using Stöber approach through adding cationic surfactant (Cetyl trimethylammonium bromide (CTAB)). Finally, the calcination process was conducted to ensure the crystallization of TiO2 shell and to remove CTAB to get mesoporous silica shell. TEM observation (Figure 2a) showed the formation of ~ 25 nm of TiO2 layer around Fe_3O_4 nanocores. TEM image (Figure 2b) revealed the

Preprints (www.preprints.org) | NOT PEER-REVIEWED | Posted: 10 August 2023 doi:10.20944/preprints202308.0829.v1

Fe_3O_4@TiO_2@m-SiO_2 structure was formed with shell thickness of 20 nm. In route R1, two different samples Fe@Ti@m-Si-0.2(R1-0.2) and Fe@Ti@m-Si-0.4(R1-0.4) we synthesized with adding 0.2 and 0.4 mL of TEOS, respectively. The thickness of shell layer was 20 and 45 nm for R1-0.2 and R2-0.4 sample, respectively.

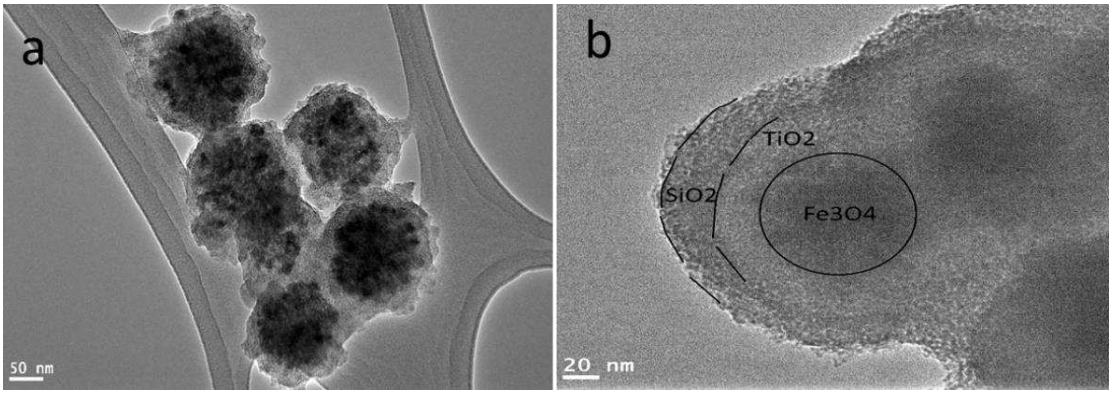

Figure 2. TEM image of (a) titania coated Fe_3O_4 nanocores and (b) Fe_3O_4@TiO_2@m-SiO_2 by first route (R1).

To fabricate Fe_3O_4core-mesoSiO_2/TiO_2 double shell using second route (sample R2), the magnetic nano-cores were subjected first to mesoporous silica coating, then to the formation of the second shell by TiO_2 coating. To achieve uniform formation of Fe_3O_4@mesoSiO_2, Stöber method in the presence of cationic surfactant was applied to form mesoporous silica layer around the magnetic nano-cores followed by titania coating as showed in Figure 3. The mesoporous silica layer is about 20 nm (Figure 3a). The second step to coat TiO_2 on the fabricated Fe_3O_4core-meso SiO_2, was achieved by hydrolysis of titanium butoxide which successfully formed a uniform 20 nm layer of TiO_2 (Figure 3b) to finally form the Fe_3O_4core-meso SiO_2/TiO_2 double shell (Figure 3). Finally calcine Fe_3O_4core-meso SiO_2/TiO_2 double shell sample at 550 ^oC was performed to crystallize TiO_2 layer and to remove surfactant in one single step.

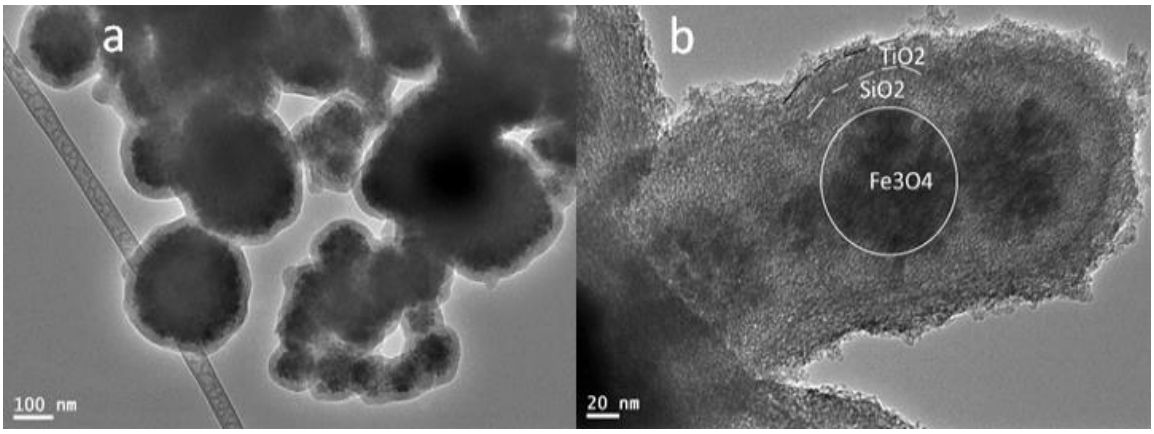

Figure 3. TEM image of (a)single shell mesoporous silica coated Fe3O4 nanocores and (b)double shell Fe3O4@m-SiO2@TiO2 by second route (R2).

N_2 adsorption-desorption isotherm was conducted for core-double shell nanoparticles prepared by route1 (at 0.2 and 0.4 ml TEOS) and route 2 at 77 K and presented in Figure 4. The prepared core-double shell derived nanoparticles even by route 1 or route 2 exhibited porous structure with type IV isotherm. It is clear that nanoparticles prepared by route 1 where silica shell is outer layer had higher surface area as well as larger pore volume (Table 1 and Figure 4A) when compared with nanoparticles prepared with route 2 where TiO_2 shell is the outer one. Moreover, these results can be explained based on porous character of silica shell compared with crystalline dense character of TiO_2 one. However, changing the silica content caused as slight increment in the surface area and pore

Preprints (www.preprints.org) | NOT PEER-REVIEWED | Posted: 10 August 2023 doi:10.20944/preprints202308.0829.v1

volume of the formed sample. Moreover, the pore size was much bigger in case of the core-double shell nanoparticles prepared by route 1 than samples of route 2 (Table 1 and Figure 4B).

Table 1. textural properties for magnetic cores-double shell prepared by route 1 and 2.

Sample	BET S. A. m^2/g	Pore volume cm^3/g	Pore size A^o
Fe@Ti@m-Si-0.2(R1-0.2)	1133.28	0.74	25.79
Fe@Ti@m-Si-0.4(R1-0.4)	1207.49	0.88	29.86
Fe@ m-Si@Ti (R2)	52.27	0.03	24.02

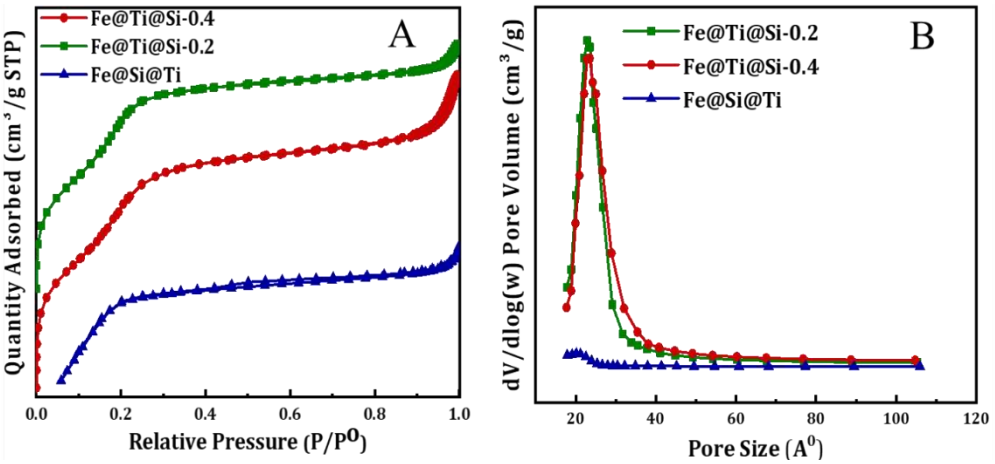

Figure 4. (A) N_2 sorption isotherm and (B) pore size distribution of calcined Fe3O4@TiO2@m-SiO2 at TEOS amount of 0.2, 0.4 mL prepared by route 1 (R1) and calcined Fe3O4@m-SiO2@TiO2 prepared by route 2 (R2).

FTIR measurements core-double shell nanoparticles prepared by route1 (at 0.2 and 0.4 ml TEOS) and route 2 (Figure 5). Si-O peak can be seen formed at 1050-1250 cm^{-1}. The Fe–O–Si peak that refer for chemical binding between Fe3O4 and silica, cannot be seen in the FTIR spectrum because it appears at around 584 cm^{-1} and therefore overlaps with the Fe–O vibration of magnetite nanoparticles. The peaks at 1632 cm^{-1} and 3425 cm^{-1} corresponding to the vibration of hydroxyl groups (-OH) on the surface of Fe3O4 nanoparticles. The peak at 970 cm^{-1} can be attributed to Ti–O–Si bond while the shoulder at 1400 cm^{-1} can be due to band to Ti–O–Ti vibration.

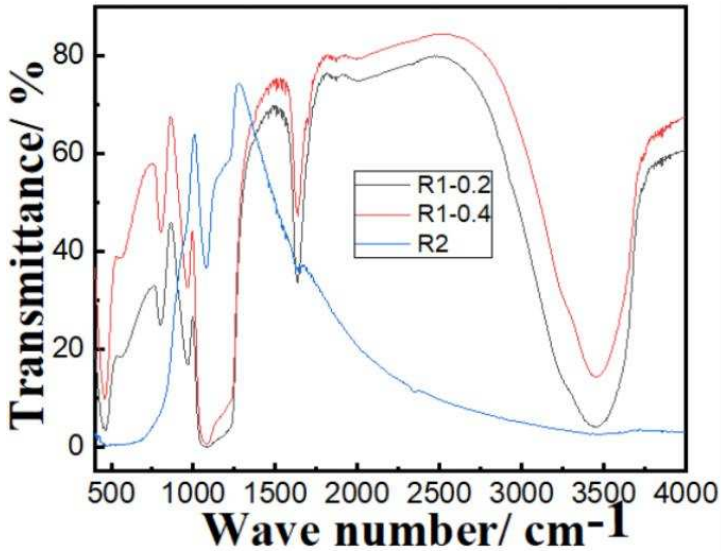

Figure 5. FTIR spectra of calcined Fe3O4@TiO2@m-SiO2 at TEOS amount of 0.2 and 0.4 mL prepared by route 1 (R1) and calcined Fe3O4@m-SiO2@TiO2 prepared by route 2 (R2).

Preprints (www.preprints.org) | NOT PEER-REVIEWED | Posted: 10 August 2023 doi:10.20944/preprints202308.0829.v1

3.2. Adsorptive-remediation investigation

Methylene blue is extensively used in the industrial section for dying and painting, resulting huge amount of colored discharge and produce many negative environmental impacts [39–41]. Herein, three adsorbent materials including the core double shell structures from R1-0.2, R1-0.4 and R2 are applied for methylene blue dyes by adsorptive-removal. The effect of the pH of the medium is investigated by varying the pH of the methylene blue sample solution from 2 to 7 (Figure 6). In the strong acidic medium the adsorption capacities for methylene blue removal using R1-0.2, R1-0.4 and R2 were in the lowest values, then increased with increasing the pH reaching its maximum value between pH 6 and 7. The lower adsorption capacity at strong pH medium may be owed to the protonation of the adsorbent surfaces [42,43].

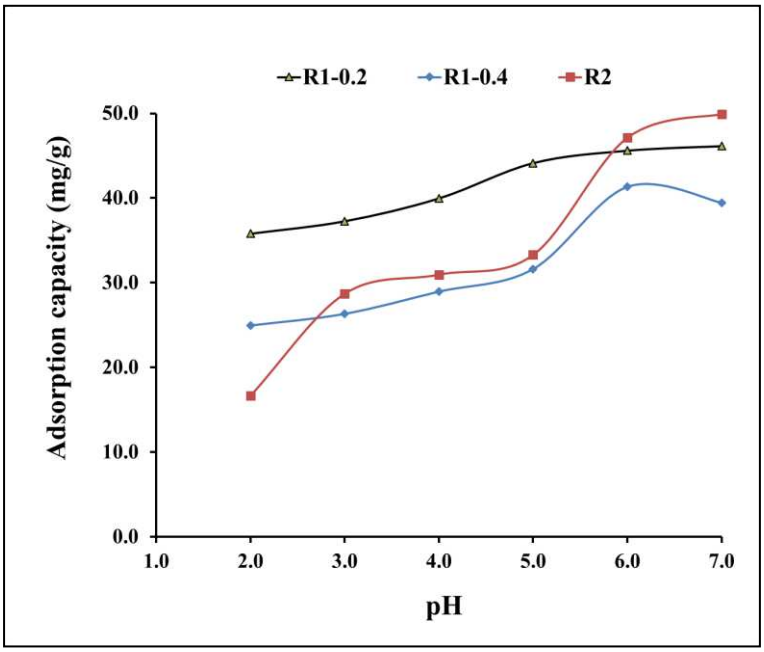

Figure 6. pH investigation for methylene blue adsorption onto R1-0.2, R1-0.4 and R2.

The effect of contact time on the de-colorization of dyes from aqueous solution by adsorption is investigated to assess the rate and efficiency of the process [44,45]. The effect of time is studied from 5 min to 180 min and the adsorption capacities for R1-0.2, R1-0.4 and R2 for methylene blue uptake are presented in Figure 7. The adsorption capacities after 1 min were 11, 9 and 15 for R1-0.2, R1-0.4 and R2, respectively, then increased till reach the equilibrium at 80 min recording adsorption capacity of 46, 38 and 50 mg/g. By increasing time from 80 min to 180 min, there are no noticeable improvement in the adsorption capacities were detected due to the occurrence of the steady state.

The rate of the mass transfer of methylene blue during adsorption process onto R1-0.2, R1-0.4 and R2 was studied by applying the kinetic models of pseudo first order and pseudo second order [46,47] as presented in Figures 8 and 9, respectively. From the data correlation, the pseudo second order kinetic model was found to be more comfortable for describing the rate of the adsorption process. The pseudo-first-order equation of Lagergren, is generally expressed in the integrated form of Equation (2):

$$\log(qe-qt) = \log qe - k1t/2.303 \quad (2)$$

By plotting log (qe − qt) versus time t, (Figure 8), The pseudo-first-order rate constant, k1, is calculated and reported in Table 2. In addition, the pseudo-second-order kinetic rate equation is expressed in the integrated form of Equation (3):

Preprints (www.preprints.org) | NOT PEER-REVIEWED | Posted: 10 August 2023 doi:10.20944/preprints202308.0829.v1

$$t/qt=1/Kqe2 + 1/qe.t \quad (3)$$

where t is the time (min), and qe (mg/g) and qe2 (mg/g) is the quantity of methylene blue adsorbed at equilibrium onto fabricated R1-0.2, R1-0.4 and R2 samples at pH 6 and 25 °C. Figure 9 present the plotting of t/qt versus t. the qe and k parameters is calculated using the slope and intercept, respectively, according to second-order kinetic model equation (3).

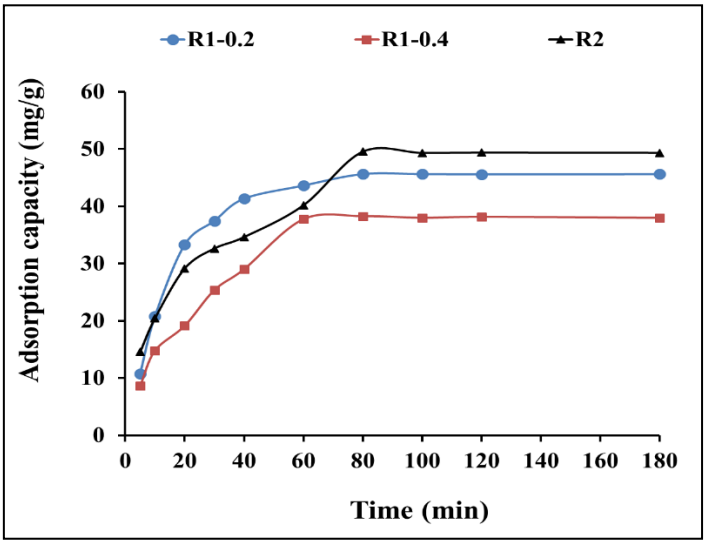

Figure 7. Time investigation for methylene blue adsorption onto R1-0.2, R1-0.4 and R2.

Table 2 shows the calculated parameters values and the linear regression correlation coefficient values. The pseudo second-order kinetic rate equation model fitting was much better than for the pseudo-first-order one. The obtained results confirm the assumption related to the second-order kinetic model including fast adsorption process. In addition, the adsorption dynamic is dependent on the migration of the methylene blue molecules to the surface of the fabricated Fe_3O_4 core-meso SiO_2/TiO_2 double shell adsorbent and finally, migration of the methylene blue molecules to the entire pores of the fabricated Fe_3O_4 core-meso SiO_2/TiO_2 double shell adsorbent [48,49].

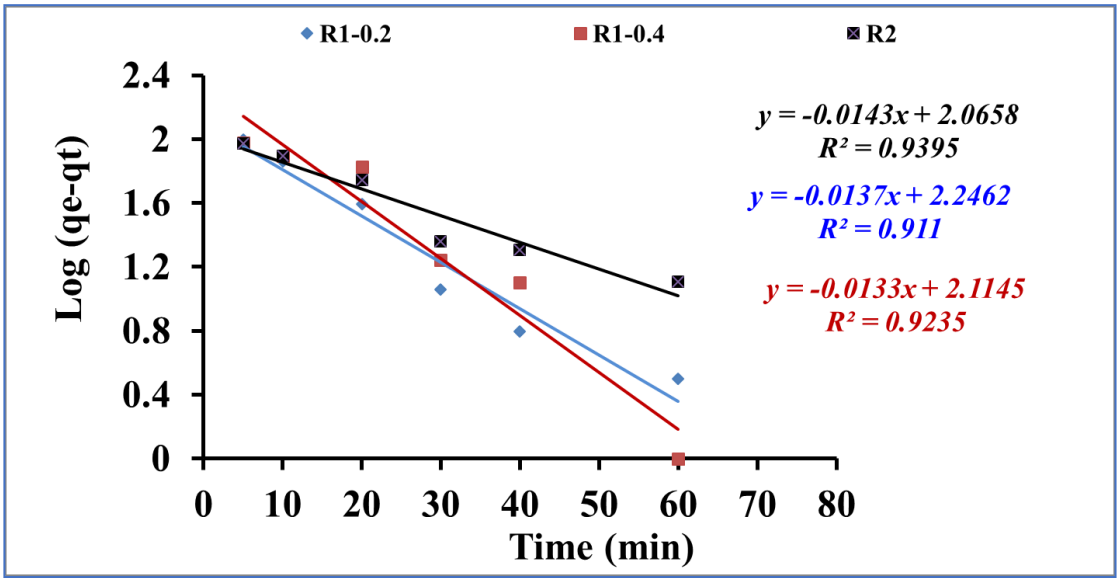

Figure 8. Pseudo first order kinetic model for methylene blue adsorption onto using R1-0.2, R1-0.4 and R2.

Preprints (www.preprints.org) | NOT PEER-REVIEWED | Posted: 10 August 2023 doi:10.20944/preprints202308.0829.v1

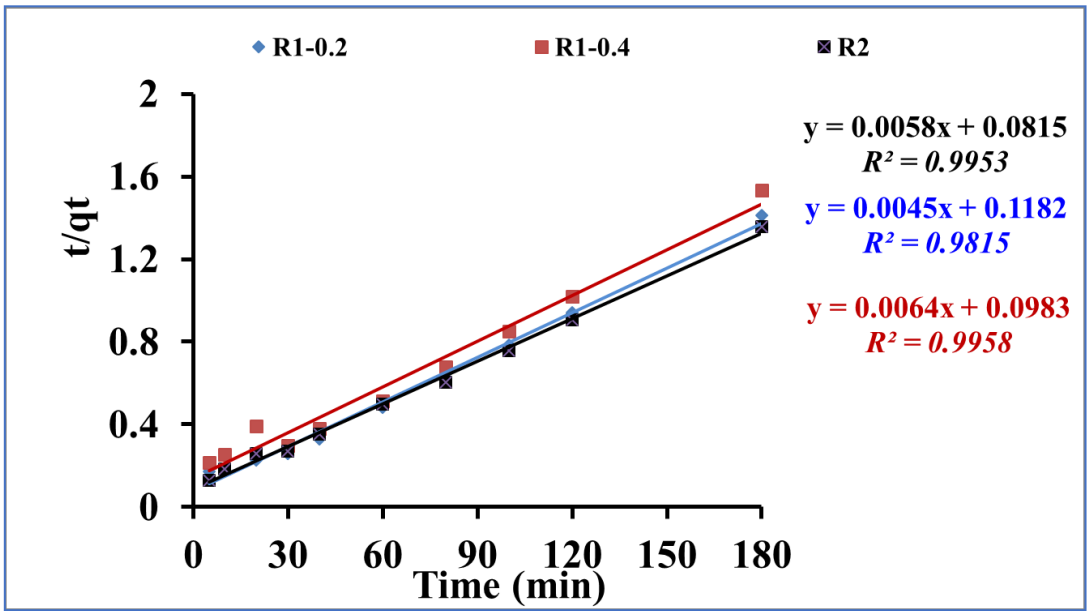

Figure 9. Pseudo second order kinetic model for methylene blue adsorption onto using R1-0.2, R1-0.4 and R2.

Table 2. Kinetic constant parameters obtained for methylene blue adsorption onto using R1-0.2, R1-0.4 and R2.

		Pseudo-First-Order			Pseudo-Second-Order		
	q_e,exp (mg/g)	K_1(min^{-1})	q_e,cal(mg/g)	R^2	k_2(g/mg.min)	q_e,cal(mg/g)	R^2
R1 -0.2	128	0.031	176.27	0.91	$1.71*10^{-4}$	222.22	0.98
R1-0.4	118	0.03	130.16	0.93	$4.16*10^{-4}$	156.25	0.99
R2	133	0.032	116.35	0.92	$4.12*10^{-4}$	172.41	0.99

3.3. Isotherms Study

The investigation of the effect of concentration of methylene blue at constant temperature (isotherms) on the adsorption capacity using fabricated R1-0.2, R1-0.4 and R2 samples is applied to assess the distribution methylene blue as adsorbate within the liquid sample solution and the solid fabricated Fe_3O_4 core-meso SiO_2/TiO_2 double shell adsorbent at the equilibrium [50–53]. The Langmuir equation (4) was used to model the adsorption data for methylene blue uptake onto fabricated Fe_3O_4 core-meso SiO_2/TiO_2 double shell adsorbent (R1-0.2, R1-0.4 and R2 samples) [54]:

$$Ce/Qe = 1/(qmax.\ b) + Ce/qmax), \quad (4)$$

where Ce is the concentration of methylene blue (mg/L) at equilibrium, Qe is the quantity of methylene blue adsorbed (mg/g), and qmax and b is Langmuir model constants (Figure 10). The correlation coefficients, R^2, for adsorption data for methylene blue adsorption onto fabricated R1-0.2, R1-0.4 and R2 samples were low, indicating that the adsorption data was not fitted by the Langmuir isotherm.

The Freundlich model assume the adsorption process occur as multi-layers of adsorbate molecules (methylene blue) onto the surface of adsorbent (Fe_3O_4 core-meso SiO_2/TiO_2 double shell). The obtained data for adsorption data for methylene blue adsorption onto fabricated R1-0.2, R1-0.4 and R2 samples were subjected to Freundlich equation [55] (Equation (5)):

$$\text{Log } qe = \log K_f + 1/n \log Ce, \quad (5)$$

Preprints (www.preprints.org) | NOT PEER-REVIEWED | Posted: 10 August 2023 doi:10.20944/preprints202308.0829.v1

where Ce is the concentration of methylene blue (mg/L) at equilibrium, Qe is the quantity of methylene blue adsorbed (mg/g). K_F (mg/g) is the Freundlich constant for the adsorbent capacity and n is related to the favorable nature of the adsorption process. Figure 11 shows the plotting of log qe and log Ce. From Freundlich equation and Figure 11 the slope and intercept indicate 1/n and log K_F, respectively.

The adsorption of methylene blue using Fe_3O_4 core-meso SiO_2/TiO_2 double shell (R1-0.2, R1-0.4 and R2 samples) showed agreement with Freundlich model (R_2>0.9) for the tested range of concentrations used in this study, suggesting multilayer adsorption process.

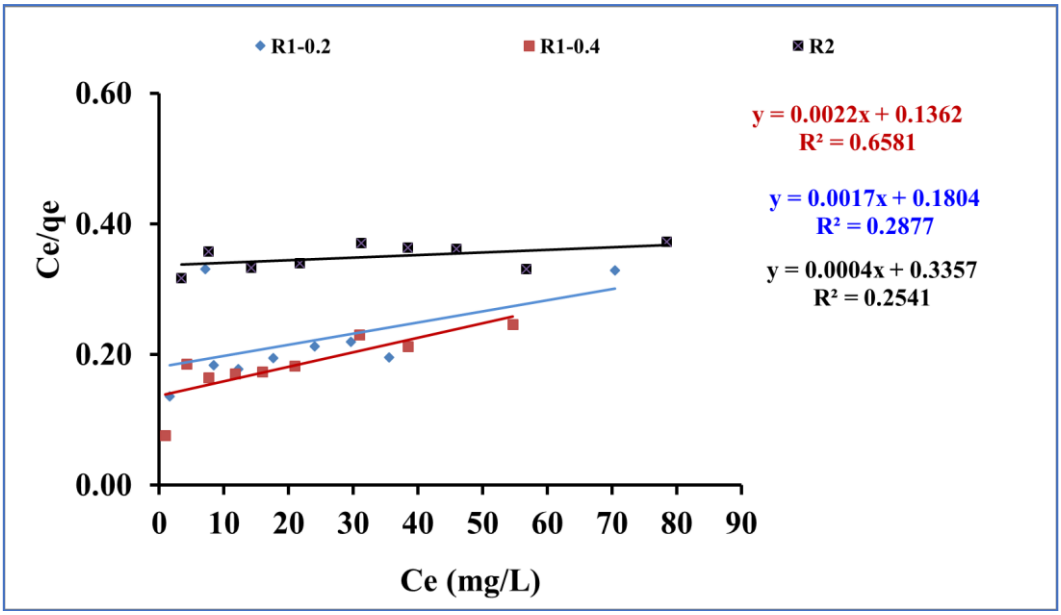

Figure 10. Langmuir for methylene blue adsorption onto using R1-0.2, R1-0.4 and R2.

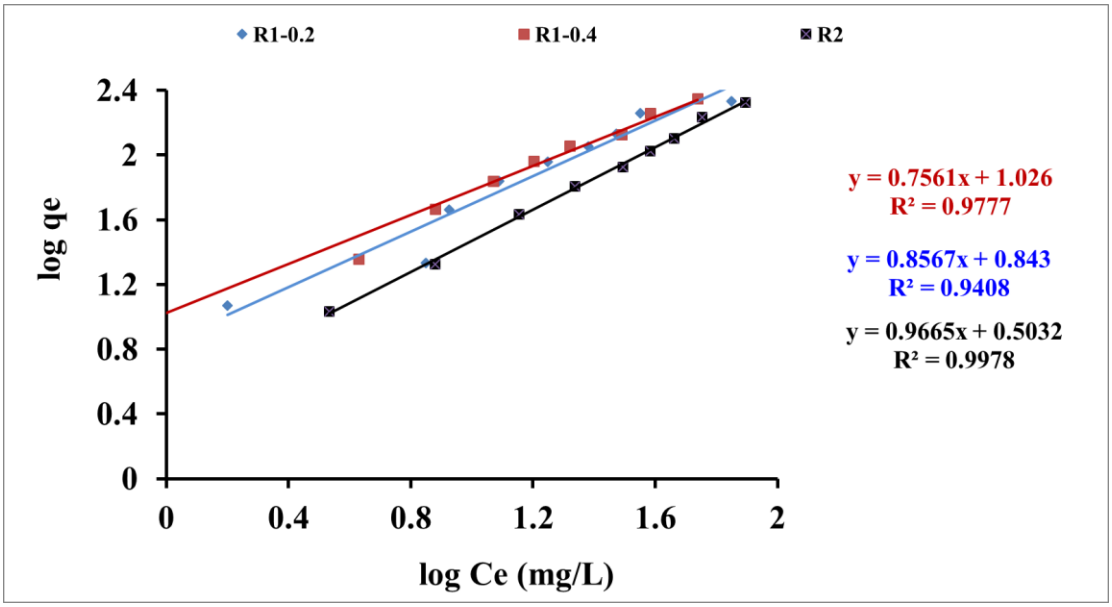

Figure 11. Freundlich isotherm for methylene blue adsorption onto using R1-0.2, R1-0.4 and R2.

Preprints (www.preprints.org) | NOT PEER-REVIEWED | Posted: 10 August 2023 doi:10.20944/preprints202308.0829.v1

Table 3. Langmuir and Freundlich parameters for methylene blue adsorption onto using R1-0.2, R1-0.4 and R2.

	Langmuir Constants				Freundlich Constants		
	K_L	b	$Q_{max.}$	R^2	K_F	n	R^2
R1 -0.2	5.54	$9.4*10^{-3}$	588.2	0.28	6.96	1.16	0.94
R1-0.4	7.34	0.016	454.5	0.65	10.61	1.32	0.97
R2	2.97	$1.19*10^{-3}$	2500	0.25	3.18	1.03	0.99

3.4. Thermodynamic Studies

Adsorption process is strongly influenced by temperature of the adsorption medium [56–58]. The temperature effect has been studied to evaluate the nature of the adsorption process of methylene blue onto fabricated Fe3O4 core-meso SiO2/TiO2 double shell. the thermodynamic parameters, including; the Gibbs free energy (ΔG°), enthalpy (ΔH°), and entropy (ΔS°) of the adsorption process of methylene blue onto fabricated R1-0.2, R1-0.4 and R2 samples are evaluated from Equations (6) and (7):

$$\log K_d = \Delta S°/2.303R - \Delta H°/2.303RT \quad (6)$$

$$\Delta G° = -RT \ln K_d, \quad (7)$$

where K_d is refer to equilibrium partition constant which is calculated as the ratio between sorption capacity of Fe_3O_4 core-meso SiO_2/TiO_2 double shell (qe) and methylene blue equilibrium concentration (Ce), R represent the gas-constant (8.314 J/mol K), and T is the temperature in Kelvin (K). From Equation (6), the plot of log K_d and 1/T (Figure 12), enable the calculation of ΔH° and ΔS° values.

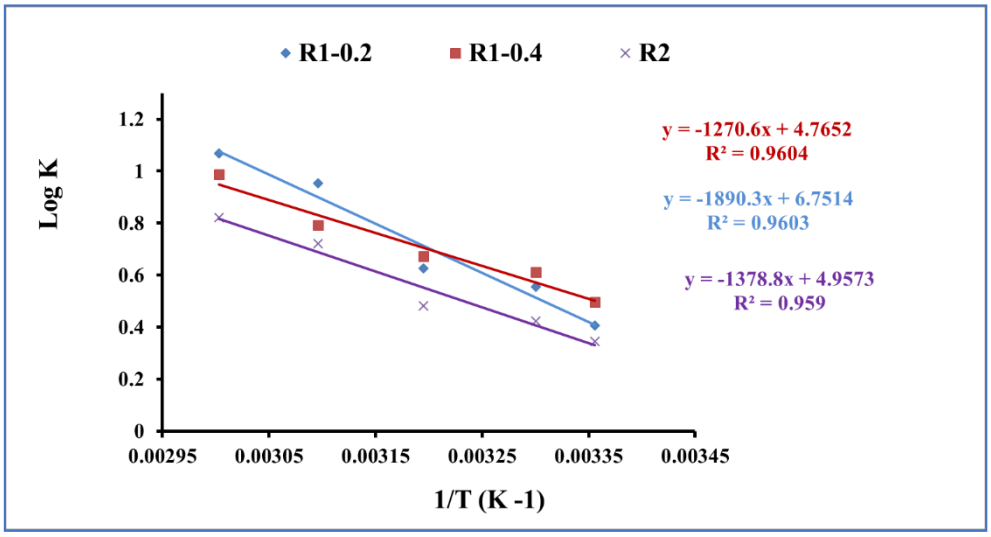

Figure 12. Thermodynamic parameters for methylene blue adsorption onto using R1-0.2, R1-0.4 and R2.

Gibbs free energy (ΔG°), enthalpy (ΔH°), and entropy (ΔS°) are presented in Table 4. ΔG◦ was obtained as negative values in the range (−2.3 to −6.8 kJ/mol) for R1-0.2, (−2.8 to −6.3 kJ/mol) for R1-0.4, and (−2.0 to −5.2 kJ/mol) for R2. In addition, the ΔH° and ΔS° values were found in the range of 26.4 to 36.19 $kJ.mol^{-1}$ and 94.9 to 126.3 $Jmol^{-1}$ K^{-1}, respectively. The calculated thermodynamic parameters indicated that the adsorption process of methylene blue onto fabricated R1-0.2, R1-0.4

Preprints (www.preprints.org) | NOT PEER-REVIEWED | Posted: 10 August 2023 doi:10.20944/preprints202308.0829.v1

and R2 samples is spontaneous with physical in nature endothermic. Furthermore, the adsorption process of methylene blue increases the degree of freedom during adsorption interaction process [59,60].

Table 4. Thermodynamic parameters for methylene blue adsorption onto using R1-0.2, R1-0.4 and R2.

	Temperature T(K)	Thermodynamic Parameters		
		ΔG° (kJ/mol)	ΔS° (J/mol/K)	ΔH° (kJ/mol)
R1-0.2	273	-2.3	**129.3**	**36.19**
	278	-3.2		
	288	-3.7		
	298	-5.9		
	308	-6.8		
R1-0.4	273	-2.8	**91.2**	**24.33**
	278	-3.5		
	288	-4.0		
	298	-4.9		
	308	-6.3		
R2	273	-2.0	**94.9**	**26.40**
	278	-2.5		
	288	-2.9		
	298	-4.5		
	308	-5.2		

4. Conclusions

Multistep fabrication processes have been investigated to fabricate Fe_3O_4 core-TiO_2/mesoSiO_2 and Fe_3O_4 core-mesoSiO_2/TiO_2 double shell nanoparticles were prepared by first (R1) and second (R2) routes as magnetic materials for adsorption of methylene blue. The TEM examination showed the successful formation of magnetic core-double shell structure including silica layer and titania layer of 20 nm thickness. The prepared magnetic core-double shell nanoparticles exhibit surface area of 1133, 1207, and 52.27 m^2/g for R1-0.2, R1-0.4 and R2 samples, respectively. The removal of methylene blue was operated at pH 6 with contact time of 80 min to reach the steady state with adsorption capacity of 46, 38 and 50 mg/g for R1-0.2, R1-0.4 and R2, respectively. Upon Applying the kinetic models, the pseudo-second-order kinetic model was well fitted with adsorption data for removal of methylene blue onto fabricated Fe_3O_4 core-TiO_2/mesoSiO_2 and Fe_3O_4 core-mesoSiO_2/TiO_2 double shell nanoparticles (R1-0.2, R1-0.4 and R2 samples). The Feundlish isotherm showed good correlation with adsorption data suggesting a multilayer adsorption. The thermodynamic parameters confirm that the adsorption process of methylene blue onto fabricated magnetic core-double shell structure is spontaneous and physical in nature.

Author Contributions: Conceptualization, Ahmed Mohamed El-Toni, Mohamed Habila and Abdulrhman Al-Awadi; Funding acquisition, Ahmed Mohamed El-Toni and Zeid ALOthman; Investigation, Ahmed Mohamed El-Toni, Mohamed Habila, Mohamed Sheikh, Mohamed El-Mahrouky and Abdulrhman Al-Awadi; Methodology, Mohamed Habila, Mohamed Sheikh, Mohamed El-Mahrouky and Zeid ALOthman; Project administration, Ahmed Mohamed El-Toni, Mohamed Habila and Zeid ALOthman; Resources, Zeid ALOthman; Supervision, Mohamed Habila; Validation, Ahmed Mohamed El-Toni, Mohamed Habila, Mohamed Sheikh, Mohamed El-Mahrouky, Abdulrhman Al-Awadi and Zeid ALOthman; Writing – original draft, Mohamed Habila; Writing – review & editing, Mohamed Habila and Zeid ALOthman.

Acknowledgments: Authors acknowledge the National Plan for Science, Technology, and Innovation (MAARIFAH), King Abdulaziz City for Science and Technology, Kingdom of Saudi Arabia for its grant with award number 14-WAT169-02.

References

1. Bonilla-Petriciolet, A.; Mendoza-Castillo, D.I.; Reynel-Ávila, H.E. *Adsorption Processes for Water Treatment and Purification*; Springer International Publishing, 2017; ISBN 9783319581361.
2. Azmi, W.; Sani, R.K.; Banerjee, U.C. *Biodegradation of Triphenylmethane Dyes*;
3. Pandey, N.; Shukla, S.K.; Singh, N.B. Water Purification by Polymer Nanocomposites: An Overview. *Nanocomposites* **2017**, *3*, 47–66, doi:10.1080/20550324.2017.1329983.
4. Yaseen, D.A.; Scholz, M. Textile Dye Wastewater Characteristics and Constituents of Synthetic Effluents: A Critical Review. *International Journal of Environmental Science and Technology* 2019, *16*, 1193–1226.
5. Ghaly, A.E.; Ananthashankar, R.; Alhattab, M.; Ramakrishnan, V. V; Ghaly, A. Ramakrishnan VV (2014) Production, Characterization and Treatment of Textile Effluents: A Critical Review. *J Chem Eng Process Technol* **2014**, *5*, 182, doi:10.4172/2157-7048.1000182.
6. Li, H. hong; Wang, Y. tao; Wang, Y.; Wang, H. xia; Sun, K. kai; Lu, Z. mei Bacterial Degradation of Anthraquinone Dyes. *J Zhejiang Univ Sci B* 2019, *20*, 528–540.
7. Lellis, B.; Fávaro-Polonio, C.Z.; Pamphile, J.A.; Polonio, J.C. Effects of Textile Dyes on Health and the Environment and Bioremediation Potential of Living Organisms. *Biotechnology Research and Innovation* **2019**, *3*, 275–290, doi:10.1016/j.biori.2019.09.001.
8. Peres, E.C.; Slaviero, J.C.; Cunha, A.M.; Hosseini–Bandegharaei, A.; Dotto, G.L. Microwave Synthesis of Silica Nanoparticles and Its Application for Methylene Blue Adsorption. *J Environ Chem Eng* **2018**, *6*, 649–659.
9. Al-Wakeel, K.Z.; Abd El Monem, H.; Khalil, M.M.H. Removal of Divalent Manganese from Aqueous Solution Using Glycine Modified Chitosan Resin. *J Environ Chem Eng* **2015**, *3*, 179–186.
10. El-Moselhy, M.M.; Kamal, S.M. Selective Removal and Preconcentration of Methylene Blue from Polluted Water Using Cation Exchange Polymeric Material. *Groundw Sustain Dev* **2018**, *6*, 6–13.
11. Liu, X.; Chen, Z.-Q.; Han, B.; Su, C.-L.; Han, Q.; Chen, W.-Z. Biosorption of Copper Ions from Aqueous Solution Using Rape Straw Powders: Optimization, Equilibrium and Kinetic Studies. *Ecotoxicol Environ Saf* **2018**, *150*, 251–259.
12. Polat, H.; Erdogan, D. Heavy Metal Removal from Waste Waters by Ion Flotation. *J Hazard Mater* **2007**, *148*, 267–273, doi:10.1016/j.jhazmat.2007.02.013.
13. Akar, S.T.; Akar, T.; Çabuk, A. Decolorization of a Textile Dye, Reactive Red 198 (RR198), by Aspergillus Parasiticus Fungal Biosorbent. *Brazilian Journal of Chemical Engineering* **2009**, *26*, 399–405, doi:10.1590/S0104-66322009000200018.
14. Dias, J.M.; Alvim-Ferraz, M.C.M.; Almeida, M.F.; Rivera-Utrilla, J.; Sánchez-Polo, M. Waste Materials for Activated Carbon Preparation and Its Use in Aqueous-Phase Treatment: A Review. *J Environ Manage* 2007, *85*, 833–846.
15. Hajeb, P.; Sloth, J.J.; Shakibazadeh, Sh.; Mahyudin, N.A.; Afsah-Hejri, L. Toxic Elements in Food: Occurrence, Binding, and Reduction Approaches. *Compr Rev Food Sci Food Saf* **2014**, *13*, 457–472, doi:10.1111/1541-4337.12068.
16. Vardhan, K.H.; Kumar, P.S.; Panda, R.C. A Review on Heavy Metal Pollution, Toxicity and Remedial Measures: Current Trends and Future Perspectives. *J Mol Liq* **2019**, *290*, 111197, doi:10.1016/j.molliq.2019.111197.
17. Qiao, W.; Zhang, P.; Sun, L.; Ma, S.; Xu, W.; Xu, S.; Niu, Y. Adsorption Performance and Mechanism of Schiff Base Functionalized Polyamidoamine Dendrimer/Silica for Aqueous Mn(II) and Co(II). *Chinese Chemical Letters* **2020**, *31*, 2742–2746, doi:10.1016/j.cclet.2020.04.036.
18. Zhan, H.; Bian, Y.; Yuan, Q.; Ren, B.; Hursthouse, A.; Zhu, G. Preparation and Potential Applications of Super Paramagnetic Nano-Fe3O4. *Processes* **2018**, *6*, 33, doi:10.3390/pr6040033.
19. López, Y.C.; Ortega, G.A.; Martínez, M.A.; Reguera, E. Magnetic Prussian Blue Derivative like Absorbent Cages for an Efficient Thallium Removal. *J Clean Prod* **2020**, doi:10.1016/j.jclepro.2020.124587.
20. Yang, J.; Hou, B.; Wang, J.; Tian, B.; Bi, J.; Wang, N.; Li, X.; Huang, X. Nanomaterials for the Removal of Heavy Metals from Wastewater. *Nanomaterials* 2019, *9*.
21. Yazdimamaghani, M.; Pourvala, T.; Motamedi, E.; Fathi, B.; Vashaee, D.; Tayebi, L. Synthesis and Characterization of Encapsulated Nanosilica Particles with an Acrylic Copolymer by in Situ Emulsion Polymerization Using Thermoresponsive Nonionic Surfactant. *Materials* **2013**, *6*, 3727–3741, doi:10.3390/ma6093727.
22. De Los Santos Valladares, L.; Bustamante Domínguez, A.; León Félix, L.; Kargin, J.B.; Mukhambetov, D.G.; Kozlovskiy, A.L.; Moreno, N.O.; Flores Santibañez, J.; Castellanos Cabrera, R.; Barnes, C.H.W. Characterization and Magnetic Properties of Hollow α-Fe2O3 Microspheres Obtained by Sol Gel and Spray

Roasting Methods. *Journal of Science: Advanced Materials and Devices* **2019**, *4*, 483–491, doi:10.1016/j.jsamd.2019.07.004.
23. S., A.J.; T., R.; Yimam, A. Magnetic Hetero-Structures as Prospective Sorbents to Aid Arsenic Elimination from Life Water Streams. *Water Science* **2018**, *32*, 151–170, doi:10.1016/j.wsj.2017.05.001.
24. Zhu, F.; Zheng, Y.M.; Zhang, B.G.; Dai, Y.R. A Critical Review on the Electrospun Nanofibrous Membranes for the Adsorption of Heavy Metals in Water Treatment. *J Hazard Mater* 2021, *401*.
25. Habila, M.A.; Alothman, Z.A.; Mohamed El-Toni, A.; Labis, J.P.; Khan, A.; Al-Marghany, A.; Elafifi, H.E. One-Step Carbon Coating and Polyacrylamide Functionalization of Fe3O4 Nanoparticles for Enhancing Magnetic Adsorptive-Remediation of Heavy Metals. *Molecules* **2017**, *22*, doi:10.3390/molecules22122074.
26. El-Toni, A.M.; Habila, M.A.; Labis, J.P.; Alothman, Z.A.; Alhoshan, M.; Elzatahry, A.A.; Zhang, F. Design, Synthesis and Applications of Core-Shell, Hollow Core, and Nanorattle Multifunctional Nanostructures. *Nanoscale* **2016**, *8*, doi:10.1039/c5nr07004j.
27. Habila, M.A.; ALOthman, Z.A.; El-Toni, A.M.; Labis, J.P.; Li, X.; Zhang, F.; Soylak, M. Mercaptobenzothiazole-Functionalized Magnetic Carbon Nanospheres of Type Fe3O4@SiO2@C for the Preconcentration of Nickel, Copper and Lead Prior to Their Determination by ICP-MS. *Microchimica Acta* **2016**, *183*, 2377–2384, doi:10.1007/s00604-016-1880-x.
28. Salamat, S.; Younesi, H.; Bahramifar, N. Synthesis of Magnetic Core–Shell Fe3O4@TiO2 Nanoparticles from Electric Arc Furnace Dust for Photocatalytic Degradation of Steel Mill Wastewater. *RSC Adv* **2017**, *7*, 19391–19405, doi:10.1039/C7RA01238A.
29. Shi, L.; Dong, B.; Gao, R.; Su, G.; Liu, W.; Xia, C.; Zhao, F.; Cao, L. Hierarchical Fe3O4@titanate Microspheres with Superior Removal Capability for Water Treatment: In Situ Growth and Structure Tailoring via Hydrothermal Assisted Etching. *RSC Adv* **2015**, *5*, 73126–73132, doi:10.1039/C5RA06362K.
30. Zheng, J.; Cheng, C.; Fang, W.J.; Chen, C.; Yan, R.W.; Huai, H.X.; Wang, C.C. Surfactant-Free Synthesis of a Fe3O4@ZIF-8 Core–Shell Heterostructure for Adsorption of Methylene Blue. *CrystEngComm* **2014**, *16*, 3960–3964, doi:10.1039/C3CE42648C.
31. Saini, J.; Garg, V.K.; Gupta, R.K. Removal of Methylene Blue from Aqueous Solution by Fe3O4@Ag/SiO2 Nanospheres: Synthesis, Characterization and Adsorption Performance. *J Mol Liq* **2018**, *250*, 413–422, doi:10.1016/j.molliq.2017.11.180.
32. Jaseela, P.K.; Garvasis, J.; Joseph, A. Selective Adsorption of Methylene Blue (MB) Dye from Aqueous Mixture of MB and Methyl Orange (MO) Using Mesoporous Titania (TiO2) – Poly Vinyl Alcohol (PVA) Nanocomposite. *J Mol Liq* **2019**, *286*, 110908, doi:10.1016/J.MOLLIQ.2019.110908.
33. Zhan, Y.; Zhao, S.; Wan, X.; He, S. Hierarchical Fe3O4-Derived Organic/Inorganic Hybrids Constructed by Modified Bio-Inspired Functionalization: Efficient Adsorbents for Water-Soluble Methylene Blue and Mechanism. *Journal of Chemical Technology & Biotechnology* **2019**, *94*, 1638–1650, doi:10.1002/JCTB.5933.
34. Schneider, M.; Ballweg, T.; Groß, L.; Gellermann, C.; Sanchez-Sanchez, A.; Fierro, V.; Celzard, A.; Mandel, K.; Schneider, M.; Ballweg, T.; et al. Magnetic Carbon Composite Particles for Dye Adsorption from Water and Their Electrochemical Regeneration. *Particle & Particle Systems Characterization* **2019**, *36*, 1800537, doi:10.1002/PPSC.201800537.
35. Akbarbandari, F.; Zabihi, M.; Faghihi, M. Synthesis of the Magnetic Core–Shell Bi-Metallic and Tri-Metallic Metal–Organic Framework Nanocomposites for Dye Adsorption. *Water Environment Research* **2021**, *93*, 906–920, doi:10.1002/WER.1481.
36. El-Toni, A.M.; Ibrahim, M.A.; Labis, J.P.; Khan, A.; Alhoshan, M. Optimization of Synthesis Parameters for Mesoporous Shell Formation on Magnetic Nanocores and Their Application as Nanocarriers for Docetaxel Cancer Drug. *International Journal of Molecular Sciences 2013, Vol. 14, Pages 11496-11509* **2013**, *14*, 11496–11509, doi:10.3390/IJMS140611496.
37. Deng, Y.; Qi, D.; Deng, C.; Zhang, X.; Zhao, D. Superparamagnetic High-Magnetization Microspheres with an Fe 3O4@SiO2 Core and Perpendicularly Aligned Mesoporous SiO2 Shell for Removal of Microcystins. *J Am Chem Soc* **2008**, *130*, 28–29, doi:10.1021/JA0777584/SUPPL_FILE/JA0777584-FILE002.PDF.
38. Li, W.; Yang, J.; Wu, Z.; Wang, J.; Li, B.; Feng, S.; Deng, Y.; Zhang, F.; Zhao, D. A Versatile Kinetics-Controlled Coating Method to Construct Uniform Porous TiO 2 Shells for Multifunctional Core-Shell Structures. *J Am Chem Soc* **2012**, *134*, 11864–11867, doi:10.1021/JA3037146/SUPPL_FILE/JA3037146_SI_001.PDF.
39. El-Ashtoukhy, E.S.Z.; Fouad, Y.O. Liquid-Liquid Extraction of Methylene Blue Dye from Aqueous Solutions Using Sodium Dodecylbenzenesulfonate as an Extractant. *Alexandria Engineering Journal* **2015**, *54*, 77–81, doi:10.1016/j.aej.2014.11.007.
40. Eslami, H.; Sedighi Khavidak, S.; Salehi, F.; Khosravi, R.; Fallahzadeh, R.A.; Peirovi, R.; Sadeghi, S. *Biodegradation of Methylene Blue from Aqueous Solution by Bacteria Isolated from Contaminated Soil*; Kurdistan University of Medical Sciences, 2016; Vol. 5;.
41. Rahman, R.; K², N.M. *DEGRADATION OF METHYLENE BLUE IN TEXTILE WASTE WATER USING ACTIVATED SAWDUST AND EGGSHELL BIOSORBENT*; Vol. 2;.

42. Yan, Y.; Zhang, M.; Gong, K.; Su, L.; Guo, Z.; Mao, L. Adsorption of Methylene Blue Dye onto Carbon Nanotubes: A Route to an Electrochemically Functional Nanostructure and Its Layer-by-Layer Assembled Nanocomposite. *Chemistry of Materials* **2005**, *17*, 3457–3463, doi:10.1021/cm0504182.
43. Karthik, R.; Muthezhilan, R.; Jaffar Hussain, A.; Ramalingam, K.; Rekha, V. Effective Removal of Methylene Blue Dye from Water Using Three Different Low-Cost Adsorbents. *Desalination Water Treat* **2016**, *57*, 10626–10631, doi:10.1080/19443994.2015.1039598.
44. Vijayalaks, G.; Ramkumar, B.; Mohan, S.C. Isotherm and Kinetic Studies of Methylene Blue Adsorption Using Activated Carbon Prepared from Teak Wood Waste Biomass. *Journal of Applied Sciences* **2019**, *19*, 827–836, doi:10.3923/jas.2019.827.836.
45. Ghaedi, M.; Nasab, A.G.; Khodadoust, S.; Rajabi, M.; Azizian, S. Application of Activated Carbon as Adsorbents for Efficient Removal of Methylene Blue: Kinetics and Equilibrium Study. *Journal of Industrial and Engineering Chemistry* **2014**, *20*, 2317–2324, doi:10.1016/j.jiec.2013.10.007.
46. AlOthman, Z.A.; Habila, M.A.; Ali, R.; Abdel Ghafar, A.; El-din Hassouna, M.S. Valorization of Two Waste Streams into Activated Carbon and Studying Its Adsorption Kinetics, Equilibrium Isotherms and Thermodynamics for Methylene Blue Removal. *Arabian Journal of Chemistry* **2014**, *7*, doi:10.1016/j.arabjc.2013.05.007.
47. Al-Othman, Z.A.; Habila, M.A.; Ali, R.; Hassouna, M.S.E.-D. Kinetic and Thermodynamic Studies for Methylene Blue Adsorption Using Activated Carbon Prepared from Agricultural and Municipal Solid Wastes. *Asian Journal of Chemistry* **2013**, *25*, doi:10.14233/ajchem.2013.14723.
48. El-Toni, A.M.; Habila, M.A.; Ibrahim, M.A.; Labis, J.P.; ALOthman, Z.A. Simple and Facile Synthesis of Amino Functionalized Hollow Core-Mesoporous Shell Silica Spheres Using Anionic Surfactant for Pb(II), Cd(II), and Zn(II) Adsorption and Recovery. *Chemical Engineering Journal* **2014**, *251*, 441–451, doi:10.1016/j.cej.2014.04.072.
49. A. Habila, M.; Sheikh Moshab, M.; Mohamed El-Toni, A.; S. Al-Awadi, A.; A. ALOthman, Z. Facile Strategy for Fabricating an Organosilica-Modified Fe3O4 (OS/Fe3O4) Hetero-Nanocore and OS/Fe3O4@SiO2 Core–Shell Structure for Wastewater Treatment with Promising Recyclable Efficiency. *ACS Omega* **2023**, *8*, 7626–7638, doi:10.1021/acsomega.2c07214.
50. Mondal, K.; Lalvani, S.B. Modeling of Mass Transfer Controlled Adsorption Rate Based on the Langmuir Adsorption Isotherm. *Sep Sci Technol* **2000**, doi:10.1081/SS-100102357.
51. Desta, M.B. Batch Sorption Experiments: Langmuir and Freundlich Isotherm Studies for the Adsorption of Textile Metal Ions onto Teff Straw (Eragrostis Tef) Agricultural Waste. *Journal of Thermodynamics* **2013**, doi:10.1155/2013/375830.
52. Moganavally, P.; Deepa, M.; Sudha, P.N.; Suresh, R. Adsorptive Removal of Lead and Cadmium Ions Using Cross-Linked CMC Schiff Base: Isotherm, Kinetics and Catalytic Activity. *Oriental Journal of Chemistry* **2016**, *32*, 441–453, doi:10.13005/ojc/320150.
53. Ayawei, N.; Ebelegi, A.N.; Wankasi, D. Modelling and Interpretation of Adsorption Isotherms. *J Chem* **2017**, *2017*, 1–11, doi:10.1155/2017/3039817.
54. Langmuir, I. THE CONSTITUTION AND FUNDAMENTAL PROPERTIES OF SOLIDS AND LIQUIDS. PART I. SOLIDS. *J Am Chem Soc* **1916**, *38*, 2221–2295, doi:10.1021/ja02268a002.
55. Freundlich, H.M.F. Over the Adsorption in Solution. *Journal of Physical Chemistry A* **1906**, *57*, 385–470.
56. Ali, I.; Alharbi, O.M.L.; Alothman, Z.A.; Badjah, A.Y. Kinetics, Thermodynamics, and Modeling of Amido Black Dye Photodegradation in Water Using Co/TiO2 Nanoparticles. *Photochem Photobiol* **2018**, *94*, 935–941, doi:10.1111/PHP.12937.
57. Ali, I.; Alharbi, O.M.L.; Alothman, Z.A.; Badjah, A.Y. Kinetics, Thermodynamics, and Modeling of Amido Black Dye Photodegradation in Water Using Co/TiO2 Nanoparticles. *Photochem Photobiol* **2018**, *94*, 935–941, doi:10.1111/PHP.12937.
58. Ghate, E.; Ganjidoust, H.; Ayati, B. The Thermodynamics, Kinetics, and Isotherms of Sulfamethoxazole Adsorption Using Magnetic Activated Carbon Nanocomposite and Its Reusability Potential. *Nanotechnology for Environmental Engineering* **2021**, *6*, doi:10.1007/S41204-021-00127-Y.
59. Othman, Z.A.A.; Hashem, A.; Habila, M.A. Kinetic, Equilibrium and Thermodynamic Studies of Cadmium (II) Adsorption by Modified Agricultural Wastes. *Molecules* **2011**, *16*, doi:10.3390/molecules161210443.
60. Habila, M.A.; ALOthman, Z.A.; Ali, R.; Ghafar, A.A.; Hassouna, M.S.E.-D. Removal of Tartrazine Dye onto Mixed-Waste Activated Carbon: Kinetic and Thermodynamic Studies. *Clean (Weinh)* **2014**, *42*, 1824–1831, doi:10.1002/clen.201300191.